

Supplementary information for

Inland advance of supraglacial lakes in north-west Greenland under recent climatic warming

Laura A. Gledhill and Andrew G. Williamson*

* *Correspondence to: A.G. Williamson (agw41@cam.ac.uk)*

Table S1. Details of the Landsat tiles (all at 30 m resolution in the optical bands) used in the study.

Satellite	Sensor	Path	Row	Tile ID	Date (DD/MM/YYYY)
Landsat-8	OLI	020	007	LC80200072016187LGN00	05/07/2016
Landsat-8	OLI	019	007	LC80190072016196LGN00	14/07/2016
Landsat-8	OLI	019	007	LC80190072016212LGN00	30/07/2016
Landsat-8	OLI	018	007	LC80180072016221LGN00	08/08/2016
Landsat-8	OLI	019	007	LC80190072016228LGN00	15/08/2016
Landsat-8	OLI	018	007	LC80180072015186LGN00	05/07/2015
Landsat-8	OLI	017	007	LC80170072015195LGN00	14/07/2015
Landsat-8	OLI	019	007	LC80180072015202LGN00	28/07/2015
Landsat-8	OLI	019	007	LC80190072015225LGN00	13/08/2015
Landsat-8	OLI	018	007	LC80180072015234LGN00	22/08/2015
Landsat 8	OLI	018	007	LC80180072014183LGN00	02/07/2014
Landsat 8	OLI	019	007	LC80190072014190LGN00	09/07/2014
Landsat 8	OLI	020	007	LC80200072014197LGN00	16/07/2014
Landsat 8	OLI	018	007	LC80180072014215LGN00	03/08/2014
Landsat-7	ETM+	019	007	LE70190072009184EDC00	03/07/2009
Landsat-7	ETM+	020	007	LE70200072009207ASN00	26/07/2009
Landsat-7	ETM+	019	007	LE70190072009216EDC00	04/08/2009
Landsat-7	ETM+	019	007	LE70190072009232EDC00	20/08/2009
Landsat-7	ETM+	018	007	LE70180072007188EDC00	07/07/2007
Landsat-7	ETM+	020	007	LE70200072007202ASN00	21/07/2007
Landsat-7	ETM+	020	007	LE70200072007218ASN00	06/08/2007
Landsat-7	ETM+	019	007	LE70190072007227EDC00	15/08/2007
Landsat-7	ETM+	018	007	LE70180072000201KIS00	19/07/2000
Landsat-7	ETM+	017	007	LE70170072000210EDC00	28/07/2000
Landsat-7	ETM+	020	007	LE70200072000215EDC00	02/08/2000
Landsat-7	ETM+	017	007	LE70170072000210EDC00	28/07/2000
Landsat-5	TM	017	007	LT50170071994185KIS00	04/07/1994
Landsat-5	TM	019	007	LT50190071994199KIS00	18/07/1994
Landsat-5	TM	018	007	LT50180071994224KIS00	12/08/1994
Landsat-5	TM	019	007	LT50190071994231KIS00	19/08/1994
Landsat-5	TM	018	007	LT50180071994240KIS00	28/08/1994
Landsat-5	TM	019	007	LT50190071990188KIS00	07/07/1990
Landsat-5	TM	018	007	LT50180071990197KIS00	16/07/1990
Landsat-5	TM	017	007	LT50170071990222KIS00	10/08/1990
Landsat-5	TM	018	007	LT50180071990229KIS00	17/08/1990
Landsat-5	TM	019	007	LT50190071988183KIS00	01/07/1988
Landsat-5	TM	018	007	LT50180071988192KIS00	10/07/1988
Landsat-5	TM	017	007	LT50170071988201KIS00	19/07/1988
Landsat-5	TM	018	007	LT50180071988208KIS00	26/07/1988
Landsat-5	TM	018	007	LT50180071988224KIS00	11/08/1988
Landsat-5	TM	018	007	LT50180071985183KIS00	02/07/1985
Landsat-5	TM	019	007	LT50190071985190KIS00	09/07/1985
Landsat-5	TM	019	007	LT50190071985206KIS00	25/07/1985
Landsat-5	TM	018	007	LT50180071985215KIS00	03/08/1985

Table S2. Annual descriptive statistics derived during the analysis of image bias towards specific periods of the melt season. n is the number of images within the year, \bar{x} is the arithmetic mean day of year of the images, and σ is the standard deviation (in days) from the arithmetic mean.

Year	n	\bar{x}	σ	Minimum day of year	Maximum day of year
1985	4	198.5	14.6	183	215
1988	5	201.6	15.6	183	224
1990	4	209.0	19.6	188	229
1994	5	215.8	23.0	185	240
2000	4	216.5	16.7	201	240
2007	4	208.8	17.3	188	227
2009	4	209.8	20.0	184	232
2014	4	196.3	13.7	183	215
2015	5	209.8	20.0	186	234
2016	5	208.8	17.1	187	228
Mean	4.4	207.6	17.3	183	240

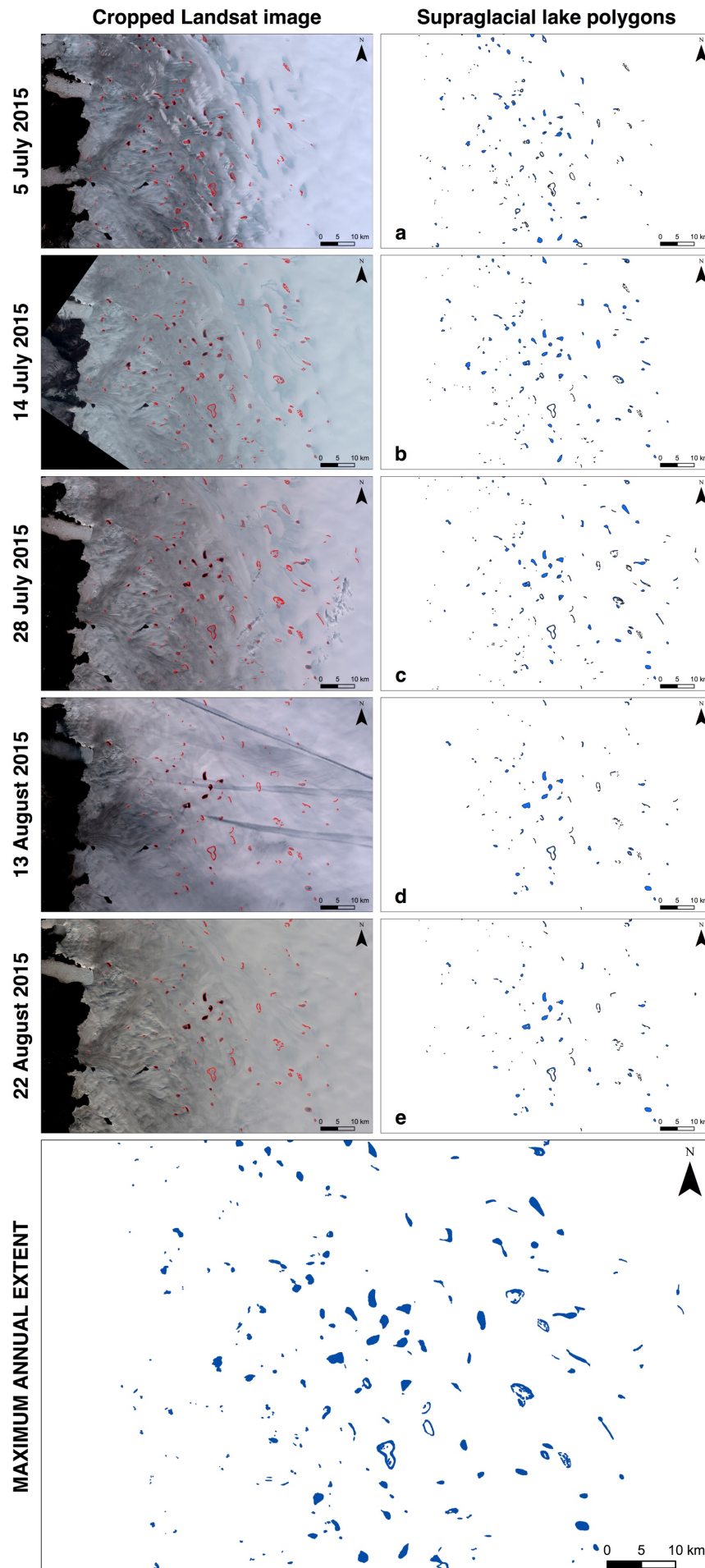


Fig. S1. Summary of the method used to derive the maximum extent of supraglacial lakes (SGLs) during July and August for each year (in this case, for 2015). SGL boundaries are delineated manually (red lines on the images) on the original cropped Landsat images (left column of panels), with the area within the boundaries then being classified as water. The individual daily masks of SGLs (blue polygons in right column of panels a–e) are then superimposed to provide the maximum extent of SGLs over July and August (blue polygons on the bottom single-column panel). Details of the Landsat images are provided within Table S1. The spatial coverage of all panels is equivalent to that shown in Figure 1.

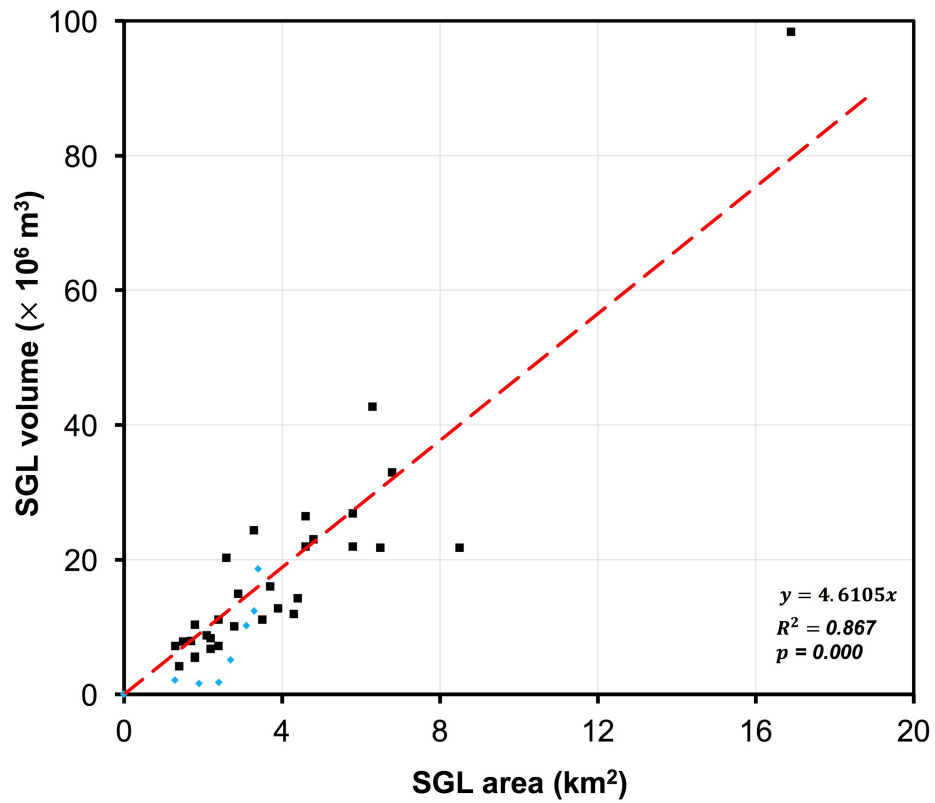


Fig. S2. The SGL area-volume scaling relationship used in the study. Blue diamonds are data taken from Georgiou and others (2009); black squares are data taken from Box and Ski (2007). The red dashed line shows an ordinary least-squares linear regression. The equation of the line and its statistical parameters are shown in the bottom right-hand corner of the graph.

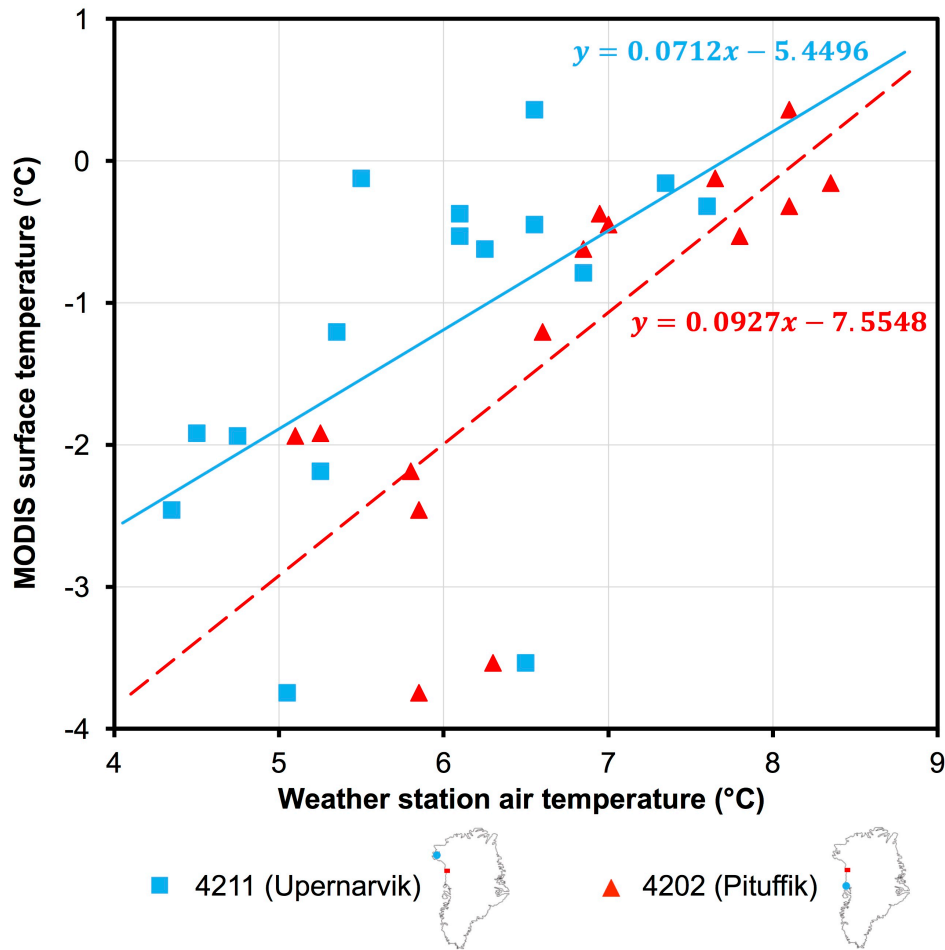


Fig. S3. The relationship between the weather station and MODIS air temperatures for the two weather stations (4211, Upernarvik; 4204, Pituffik) considered for use in the study (Cappelen and others, 2015) during the overlapping years (2000–2015 for Pituffik and 2000–2014 at Upernarvik). The solid blue line shows an ordinary least-squares linear regression applied to the Upernarvik and MODIS data ($r = 0.772$; $R^2 = 0.596$; $p = 0.01$); the dashed red line shows an ordinary least-squares linear regression applied to the Pituffik and MODIS data ($r = 0.555$; $R^2 = 0.308$; $p = 0.260$). Equations for both lines are shown on the graph (blue and red text, respectively). Insets show the locations of the two weather stations within Greenland (blue dots) relative to the study site (red square) to highlight their similar spatial proximity to it.